RECOVERING CLIMATE SIGNALS FROM TREE-RING COLOR IN THE DRY SIERRA NEVADA OF CALIFORNIA

A Thesis submitted to the faculty of
San Francisco State University
In partial fulfillment of
the requirements for
the Degree

Master of Science

In

Geoscience

by

Natasha Tarra Fazeli

San Francisco, California

August 2020

CERTIFICATION OF APPROVAL

I certify that I have read RECOVERING CLIMATE SIGNALS FROM TREE-RING COLOR IN THE DRY SIERRA NEVADA OF CALIFORNIA by Natasha Tarra Fazeli, and that in my opinion this work meets the criteria for approving a thesis submitted in partial fulfillment of the requirement for the degree Master of Science in Geoscience at San Francisco State University.

Alexander Stine, Ph.D.
Associate Professor

Petra Dekens, Ph.D.
Professor

Kevin Simonin, Ph.D.
Associate Professor

RECOVERING CLIMATE SIGNALS FROM TREE-RING COLOR IN THE DRY SIERRA NEVADA OF CALIFORNIA

Natasha Tarra Fazeli
San Francisco, California
2020

Tree rings form an important part of our observing network for surface climate before the introduction of widespread instrumental observation. Tree rings produce annual climate reconstructions and outnumber other paleoclimate proxies. In most regions of California tree ring width correlates positively with seasonal precipitation amount. The blue intensity tree ring proxy has gained increased attention because of the potential to capture much of the climate signal typically recovered by density proxies, with lower costs and a shorter processing time. Studies of both blue intensity and latewood density proxies are strongly concentrated in temperature stressed regions, and little is known about how these proxies perform in moisture stressed environments. In this study, we investigate the climate signals recorded in blue intensity and tree ring width for Ponderosa and Jeffery Pines sampled at sites along a transect through the Sierra Nevada Range, with sites spaced across a gradient of hydrological stress regimes. A total of 8 sites were sampled, with 304 cores taken between 37.3 north and 39.6 north. With 5 sites currently analyzed, all 5 show tree ring width to be positively correlated with annual mean (Sep*-Aug) rainfall, reflecting the large-scale arid climate of the region. The strength of this correlation decreases with elevation, ranging from R=0.54 at our lowest elevation site (700 meters elevation on western side of Sierra Nevada), to R=0.15 at our highest elevation site (2300 meters elevation also on western side). Despite the large-scale moisture-limitation regime, we find a positive relationship between blue intensity and growing season (Jun-Aug) temperature at 3 of our 5 analyzed sites. There is no apparent relationship between the strength of this relationship and elevation. We find limitations in reconstructing temperature at our 2 northern study sites, where we found a positive relationship between blue intensity and annual mean (Sep*-Aug) rainfall. We hypothesize that it will be possible to use blue intensity in conjunction with tree ring width across a gradient of moisture stress regimes to simultaneously estimate paleotemperature and paleomoisture in the California Sierra Nevada.

I certify that the Abstract is a correct representation of the content of this thesis.

Chair, Thesis Committee Date

PREFACE AND/OR ACKNOWLEDGEMENTS

I am so privileged to have had the opportunity to complete such an immense study. First, I’d like to thank my advisor and wilderness guide Dr. Alexander Stine. A Master’s Thesis is really a partnership between a student and their mentor, and I was so lucky to have such an intelligent and helpful advisor to take my project from idea to reality. So many thanks to Dr. Petra Dekens and Dr. Kevin Simonin, my committee members, for guiding me with their unique insight on my project. I can’t emphasize enough how important my partner Erik Phillips was in completing this project. He may not have shared my passion for dendrochronology, but he was vital in helping with the collection of my samples. Additionally, I appreciate my family and friends for going on this journey with me, with their emotional support. This project was changed to a small extent due to COVID-19, as many things were in 2020. I am so lucky to have been safe and able to complete my thesis.

TABLE OF CONTENTS

LIST OF TABLES

LIST OF FIGURES

INTRODUCTION

From the formation of this planet to the Holocene epoch, climate has fluctuated due to environmental factors. Recently, anthropogenic climate change has increased global temperatures and is projected to cause extreme variability between weather events. Paleoclimate provides a context for future climate change, however it is limited by temporal availability of in situ climate measurements prior to the 19th century. In order to understand past climates we can use proxies, which trace environmental conditions and can be indicators of past climate. An example of one of these proxies is tree ring width, which is the average length of lateral ring growth in a single year from a group of trees. Since tree growth occurs annually, the Intergovernmental Panel on Climate Change has used tree rings for a global climate reconstruction (IPCC Report 2018). Tree ring studies are the most important paleoclimate records for studying climate change as their datasets outnumber all other paleoclimate proxies (Bjorklund et al. 2019). We know that there is a warming trend globally and locally in California, but our California temperature record is short, so we need other tools besides in situ data to extend the temperature record.

Tree ring width studies in the mesic Sierra Nevada have included studies on the association between ring width and temperature (Scuderi 1993; Graumlich 1993; Millar et al. 2004; Bunn et al. 2005; Kipfmueller and Salzer 2010; Dolanc et al. 2013), precipitation (Graumlich 1993; Cook et al. 2004; Bunn et al. 2005; Kipfmueller and Salzer 2010; Dolanc et al. 2013), competition (Johnson et al. 2017; Ma in review), and fire history (Brown et al. 1992). In the past millennium we have seen megadroughts in California, which were discovered using trees to recreate rainfall (Cook et al. 2004). In order to model temperature from tree rings in the Sierra Nevada, researchers have used samples from trees at or near treeline. Here we are attempting to determine temperature from trees at a variety of elevations, including those far below treeline. I am exploring the hypothesis that some aspects of tree growth are responding to temperature; in this study we are using latewood color as a proxy, titled blue intensity. If this is true it would allow us to reconstruct past temperature annually in California.

Research Questions

In this study we completed a transect across the Sierra Nevada to address two questions: Does tree ring width and blue intensity permit quality reconstruction of precipitation and temperature variability, respectively, at sites in arid California? How does the temperature signal in blue intensity and the precipitation signal in tree ring width vary with distance to treeline? We hypothesize that if these results can be replicated at locations near and far from treeline, then both tree ring metrics of tree ring width and blue intensity can be used in reconstructions for a wider view of climate in arid zones.

BACKGROUND

Tree Growth

Cells in an annual growth ring contribute to tree mechanics (Fig. 1). Tree growth occurs in annual rings made up of tracheid cells and parenchyma cells (Rathgeber et al. 2016). Tracheid cells are used for water transport and mechanical support in trees (Cuny et al. 2014). A matured and deceased tracheid has an empty area within the cell which is called the lumen, and surrounding the lumen is the cell wall. The size of the lumen area and the thickness of the cell wall are dependent on the climate conditions the tree experiences.

The growth of a tree depends on its local environmental conditions, including nutrients, water, light availability, and temperature conditions (Fritts et al. 1991; Stine and Huybers 2014). At the base of a mountain, higher temperatures and decreased rainfall causes radial tree growth to be typically moisture limited, which can transition to temperature limitation with increased elevation. Treeline is a figurative contour at high elevation on a mountain where temperature limitation overcomes tree growth. Here we find trees whose radial growth is limited by temperature so extremely that temperature normally outweighs other environmental stressors (Fritts et al. 1976). California is comprised of mostly moisture limited environments, so a transect at the same latitude from the base of the Sierra Nevada to treeline should encompass a range of morphological stressors.

The two dominant frameworks for understanding how climate can influence tree growth rate at a large scale are known as source limitations and sink limitations. The argument that the sink mechanism limits plant growth asserts that environmental conditions limit plant growth, therefore climate controls the rate at which trees use surrounding resources to grow (Rathgeber et al. 2016). The source mechanism purports that photosynthesis, as in available resources such as carbon, limits plant growth (Rathgeber et al. 2016). Climate is the controlling factor for what resources are available for the tree in any given year. For the purpose of interpreting the results of this study we are assessing the relevance of each of these mechanisms for modulating lumen area size and cell wall thickness in latewood.

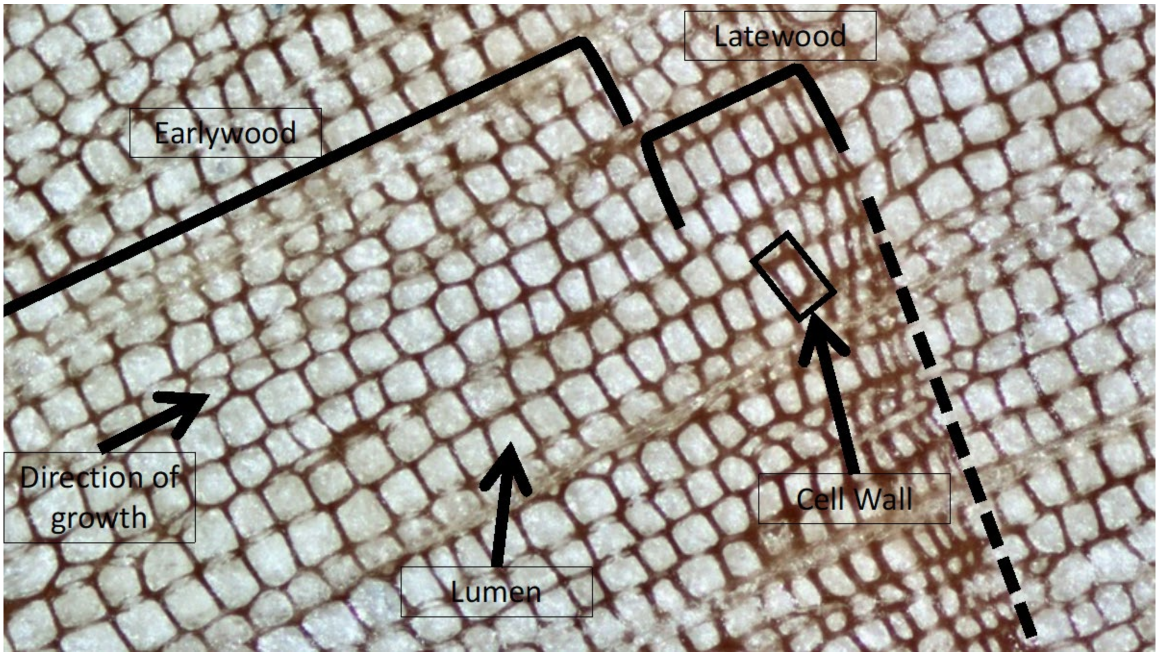

Figure 1 High resolution image of a *Pinus Ponderosa* cross-section.

Sample taken from site GRM. Individual cells from the bottom left to the top right in the tree ring show the transition from earlywood to latewood, with the year of growth ending at the dashed line. Relevant ring structure elements are highlighted, including a lumen and a cell wall.

Tree Ring Structure

Within a year of growth, a tree will produce both earlywood and latewood (Fig. 1). Earlywood is the portion of the tree ring that appears lighter in color due to large lumina and thinner cell walls in the tracheid cells, which holds the primary function of transporting water in the tree (Bjorklund et al. 2017, Fonti et al. 2013). Latewood is the darker portion of the ring that is characterized by smaller lumina and thicker tracheid cell walls, which provides more of the mechanical support for the tree (Bjorklund et al. 2019, Fonti et al. 2013). Cell formation occurs during the summer season in extratropical regions, and switches from earlywood to latewood around the beginning of summer (Rathgeber et al. 2016). Understanding tree structure at the cellular level can increase our understanding of how the various aspects of tree rings can record climate.

Tree Ring Proxies

Tree Ring Width (TRW) is by far the most widely used tree-ring proxy and has been used to make inferences about past climate for over 50 years (Fritts 1966). The width of a ring largely depends on the amount of cells produced in a year (Bjorklund et al. 2017). In previous studies, TRW has had a strong positive relationship with temperature (Schweingruber et al. 1978, Briffa et al. 1998, Briffa et al. 2002, Bunn et al. 2011, Johnson et al. 2011, Vaganov et al. 2011, Bjorklund et al. 2017, Wilson et al. 2017, Ma et al. *in review*), and with precipitation (Schweingruber et al. 1978, Bunn et al. 2011, Griffin et al. 2011, Johnson et al. 2011, Dannenburg and Wise 2016). TRW often only provides reconstruction of moisture, so other measurements of climate in trees have been explored to reconstruct temperature in arid environments (Bjorklund et al. 2014).

In addition to measuring TRW, we can infer past climate variability in tree rings by using x-ray images or light reflectance to determine the density of latewood tracheids. Optical proxies use the coloring of the lignin in the latewood cell walls of a tree ring for determining climate conditions (Campbell et al. 2007). The darkness of the latewood changes from ring to ring, which depends on the size of tracheid lumina and the thickness of cell walls (Bjorklund et al. 2017). Warmer temperatures lead to thicker cell walls in latewood and smaller cell lumen, which darkens latewood, traditionally found in temperature-limited regions across the extra-tropical Northern Hemisphere (Briffa et al. 2002, Fonti et al. 2013). The blue color channel was found empirically to work the best (McCarroll et al 2002), so optical proxies using blue reflectance to determine climate have been termed Blue Intensity (BI). In temperature-limited environments, BI is a better proxy for temperature than tree ring width (Bjorklund et al. 2014), and it has similar results as x-ray imaging.

The original tree ring proxy for determining density is called maximum latewood density (MXD), and it is a common proxy for temperature using tree rings (Schweingruber et al. 1978, Briffa et al. 2002, Campbell et al. 2007, Bjorklund et al. 2013, Bjorklund et al. 2015, Bjorklund et al. 2014, Rydval et al. 2014, Bjorklund et al. 2017, Bjorklund et al. 2019). Because of the difficulty and cost of measuring tree-ring density, its use is restricted to a few research laboratories, all located in Europe. MXD is prepared by taking a measurement of the highest density of the latewood region with x-rays, which is compared to climate for that year (Björklund et al. 2013). MXD and optical proxies are closely tied, since both use the latewood portion of a tree ring to reconstruct climate, and with nearly matching results in decadal timescales (Bjorklund et al. 2014). In regions that are broadly temperature limited, both proxies have been used to reconstruct temperature (Wilson 2017). Optical proxies are less time-consuming than MXD, and due to their low cost and ease of access, can be used across the globe.

Mechanisms of Tree Ring Formation

Previous evidence suggests that year-to-year variability in MXD is broadly controlled, across northern high latitudes, by variability in cell wall thickness governed by temperature stress variability. By extension, we expect that maximum latewood BI would also be controlled in these regions by temperature, at least to the extent that BI and MXD measure the same tree ring component.

Direct measurements of year-to-year variability of cell wall thickness and lumen area in conifers show that latewood density variability is driven by cell wall thickness. The most direct study to investigate this relationship considered measurements of cell anatomy geometry from 349 tree ring chronologies from 1901 to 2013 across the Northern Hemisphere (Bjorklund et al., 2017). Various tree density and width parameters were compared to climate for correlation analysis. Based on measurements of cell wall thickness and cell lumen size, they calculated the density variation that would arise due to only variation in cell lumen size (ρ_{lumen}) from variations in cell wall thickness (ρ_{wall}) and due to variation in both (ρ_{true}). It was found that interannual variability of latewood density (ρ_{true}) was positively correlated with predictions based on cell wall thickness ($R(\rho_{true}, \rho_{wall}) = 0.65$), but negatively correlated with predictions based on lumen size ($R(\rho_{true}, \rho_{lumen}) = -0.45$). The negative correlation between predictions based on lumen size and density is possible because the predictions made based on lumen size and cell wall thickness are so strongly anti-correlated ($R(\rho_{lumen}, \rho_{wall}) = -0.95$). We take this as strong evidence that interannual latewood density variability is widely controlled by cell wall thickness variability. We do note that this study drew on trees from throughout the Northern Hemisphere and may or may not reflect the mechanisms present at the sites used in this thesis.

There is strong evidence at high latitudes that MXD is controlled by temperature. In temperature-limited regions across the extra-tropical Northern Hemisphere, interannual tree growth for conifers from 387 sites were compared to climate (Briffa et al., 2002). At all locations TRW and MXD were positively correlated with summer temperature, with a more steady correlation between MXD and temperature ($R>0.22$ at 90% of sites). In cold environments where TRW has a positive relationship with temperature, they find that TRW is positively correlated with MXD (Bjorklund et al., 2017). In principle, a positive correlation between temperature and MXD could arise because temperature forces evaporation, and so is associated with moisture stress. However, if this were the case one would expect to see negative correlation between precipitation and MXD beyond the correlation that is necessitated by the relationship between temperature and MXD. This is not seen in the Briffa et al., 2002 study.

Mechanistic arguments exist as to why temperature variability can contribute to variability in cell-wall thickness. Cell wall lignification helps turn cells into “pipes” for transporting water, and this process is limited by temperature (Rathgeber et al., 2016). Warmer weather in temperature-limited environments increases lumen size, which in turn results in cells with more capacity to transport water, and therefore increases carbon assimilation for thickening cell walls (Fonti et al., 2013). Therefore, temperature determines MXD, and by extension BI, in cold environments in the Northern Hemisphere.

Blue Intensity Determines Past Temperature

The BI proxy has been used most often throughout Europe to reconstruct summer temperatures, but there is a knowledge gap in how BI responds in Mediterranean climates where moisture limits growth (Fig. 2). BI from latewood has been used to reconstruct temperature (Campbell et al. 2007, Bjorklund et al. 2013, Rydval et al. 2014, Bjorklund et al. 2015, Wilson et al. 2017, Bjorklund et al. 2019) and precipitation (Dannenburg and Wise 2016). Due to the absence of data in arid regions, there is a lack of information about what optical proxies record in the western United States.

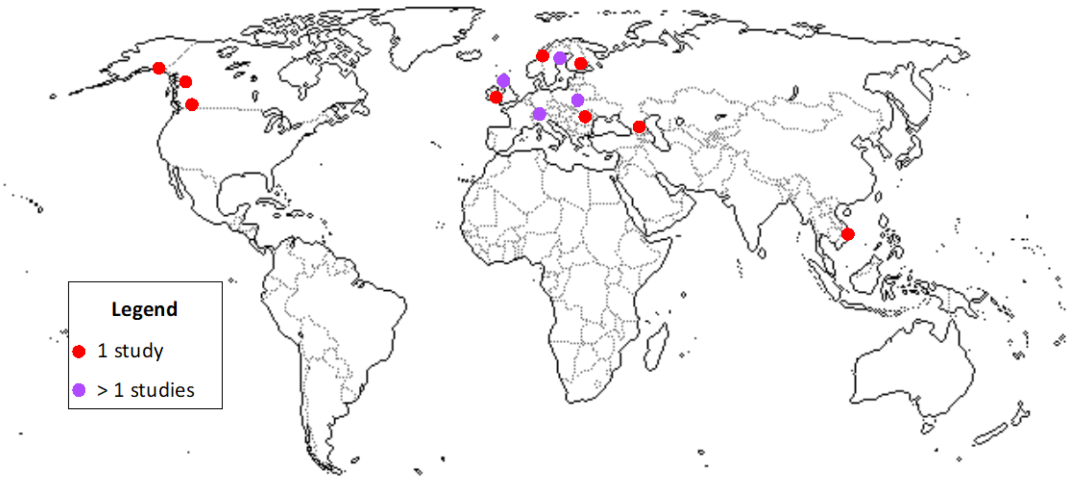

Figure 2 Location of past blue intensity studies.

Map of continents and countries, where red dots indicate the location of one blue intensity study, and purple dots indicate a location with many blue intensity studies. No blue intensity study to date has been conducted in Mediterranean climates or in the continental United States.

METHODS

Site Locations

Our goal was to explore the sensitivity of the blue intensity proxy at a variety of temperature and moisture limited sites. We originally found interesting results at a single location in the foothills of the Sierra Nevada, and from there we chose sites nearby with increasing elevation on the west side and with decreasing elevation down the east side. We sampled two closely related tree species for this study, Ponderosa Pine (*Pinus Ponderosa)* and Jeffrey Pine (*Pinus Jeffreyi)*. To understand climate information from tree rings, we collected, prepared, and analyzed tree cores. Site selection for this study's sampling was based on the presence of the desired species population and specific elevation, including locations from the foothills to near treeline.

We sampled trees at eight sites across the Sierra Nevadas at a variety of elevations (Fig. 3, Table 1). The first three sampling sites were in or near Stanislaus National Forest, the next two were on the eastern side of the Sierra Nevadas in Humboldt-Toiyabe National Forest, and the last three were northern sites, in Tahoe National Forest. The original site is in the foothills of the Sierra Nevadas where 26 *P. Ponderosa* were sampled at a private residence in Oakhurst, CA (Carver et al. 2018). Grandma (GRM) site is at 800 meters elevation and experiences a Mediterranean climate. North Round Strawberry (NRS) is located just barely northwest of the city of Strawberry on California Highway 108 on relatively flat land and at 1700 meters elevation. The NRS site is in

Stanislaus National Forest, and showed evidence of recent logging. North Deadman's Switchback (NDS, Fig. 4) is located on California highway 108, north of Deadman Creek, uphill on a slope at about 15 degrees, at 2300 meters elevation. The 51 *P. Ponderosa* sampled at this site in Stanislaus National Forest were among the oldest trees we sampled, up to 330 years old. On the east side of the Sierra Nevadas in Humboldt-Toiyabe National Forest is the Sonora Bridge Campground (SBR) site, which is on a hill with a plateau top next to the campground of the same name. The site was chosen as it looked as though it had a cluster of trees on the top of the hill when looking from below. The slopes of the hill were steep but the trees that were sampled at the top were on somewhat flat land. While still in Humboldt-Toiyabe National Forest on the east side of the Sierra Nevada we sampled at a site with a slightly lower elevation than SBR. In the north, the BWF site is located in Tahoe National Forest off of California highway 49 at 1600 meters elevation. At this site we sampled Ponderosa Pine, Incense Cedar, and Sugar Pine, but only *P. Ponderosa* samples were analyzed for this study. The Sierra Nevada Field Campus site (SNF) is located on San Francisco State University property in Tahoe National Forest in Sierra City off California highway 49 at 1700m elevation. The *P. Ponderosa* cores were taken on the hill slope just south of the buildings on the campus. Samples at SNF were taken on a slope of about 30 degrees. Sites BWF and SNF are within 5 km of each other, with only 8 cores in the SNF chronology, so we have considered combining these two sites into one single site. Our YPS site is located in

Tahoe National Forest at 2100 meters elevation with only White and Red Fir collected, so those samples are not included in this study.

Figure 3 Locations of sites in transect.

All eight locations sampled indicated by circles and triangles on satellite map of California. Circles indicate site locations that are included in the analysis of this thesis, while triangles indicate site locations not included yet.

Figure 4 Photo at site NDS.

View is looking south and downslope towards Highway 108. Ponderosa Pine are the most visible trees in photo.

Sampling Protocol

To have enough cores for climate reconstruction, our goal was to collect 20-60 tree cores, per site. A portion of the trees we cored are sampled twice in order for crossdating later in the process. We used Haglof increment bores to drill from the bark to the pith at breast height for approximately 30 trees per site, with one to two cores taken per tree, drilling perpendicular to slope (Fig. 5). Cores were placed into paper straws which have the core code and any relevant notes written on them, including, but not limited to, tree species, GPS point, name of sampler, date, cardinal direction on the tree where the bore was drilled, cardinal direction of the slope, and approximate age. We took a total of 304 cores, with 198 included in the analysis of this study.

Figure 5 Hagloff increment borer and Pinus ponderosa core.

Resin Extraction

In order to separate accurate BI values from accumulated resin in the core, age-related staining must be removed (Björklund et al. 2015). We followed procedures set by Milos Rydval using 99% acetone to remove resin. After collecting cores from the field and bringing them back to the lab, we allowed the cores to dry for at least one week before starting to process them. First, we removed the core from the straw and recorded its length and straw information, then we took a picture of the core and straw against a ruler. In order to identify the core later, we used a pencil to write the core code every few centimeters across the core, and if it was fragmented we used arrows and letters to connect the core back together in the future, if the pieces were separated. Using metal wires, we connected 5-6 cores around a metal rod and placed several bundles in a 2000 ml cylinder. In a fume hood, we poured as much acetone as is necessary to completely cover the cores, with additional acetone to account for evaporation. We then wrapped the top with plastic wrap and sealed the cylinder with a cap, followed by more plastic wrap and tape in order to create seal as close to airtight as possible (Fig. 6). The cores were removed after 72 hours of soaking and left to dry for at least 24 hours in the fume hood. While most of the collected cores went through this process, we did not have a wet lab set up at the beginning of this study, so not all of the cores were processed with resin extraction. Of those sites included in this study, NRS and NDS cores had extractives removed, while BWF, SNF, and GRM cores did not (Table 1).

Figure 6 Original setup for resin extraction.

Cores are measured and labeled, connected around a metal rod with acetone-safe zip ties, and then soaked in acetone for 72 hours in a sealed container. Later versions used a 2000 ml beaker, to hold more cores, and plastic wrap to ensure a more secure seal.

Mounting and Sanding

In order to measure the samples digitally, the cores must be sanded to create a flat surface for and capture cellular resolution. To accomplish this, we took the resin extracted cores and mounted them on wooden mounts. The wooden mounts were custom made to fit our size core cylinders. The cores were glued down on the mounts with the radial direction upright on the mount. It is important that the core is not twisted in order to measure radial width accurately. After mounting, the cores were sanded with an electric belt sander several times, with 240, 400, 600, and 800 grit sand paper, in that order. The sanding is completed in order to make cellular resolution visible and flatten the surface for scanning. Next, the sanded cores were scanned with a high-resolution scanner, an Epson Expression 11000XL photo scanner, in order to measure TRW and BI digitally.

Measuring Samples, Crossdating, & Establishing Site Chronologies

To measure TRW and BI on each ring of a core we used CooRecorder, a computer program (Larsson 2013). Cores were cross-dated in CDendro and COFECHA (Holmes 1983) with other samples from the same site in order to account for missing rings or false rings. False rings are defined as sections of smaller cell lumen during periods of seasonal drought or moisture stress, and are features that can be mistaken for new annual growth (Griffin et al. 2011, Babst et al. 2016). During the cross-dating process, we found a few cores at each site that do not match the common climate signal coming from the site, so those were left out of the final chronology.

As trees age, non-climatic conditions adjust the ring size, so the process of de-trending is done to remove age-growth effects (Campbell et al. 2007). Detrending removes the age trend from the individual tree in order to highlight the common climate signal in all trees at a site. We used a negative exponential function as the growth curve, which uses the following equation: $f(i) = a*exp(-b*t(i)) + d$. To standardize and create a tree ring index, the tree ring widths are divided by this growth curve at each point. The TRW and BI measurements were each turned into chronologies using the program ARSTAN, which detrends the individual trees and compiles them. The program returns datasets which have one measurement for each year (Cook 1985).

TRW and BI data was compared to climate data from Climatic Research Unit Time-Series version 4.03 (CRU TS4.03) in 0.5x0.5-degree gridded data sets (Fig. 7). The monthly average temperature and monthly summed precipitation datasets span from 1901-2018, depending on when the individual site was sampled. All sites experience large variance in both precipitation and temperature throughout the year, while the maximum winter precipitation is decreased at northern sites.

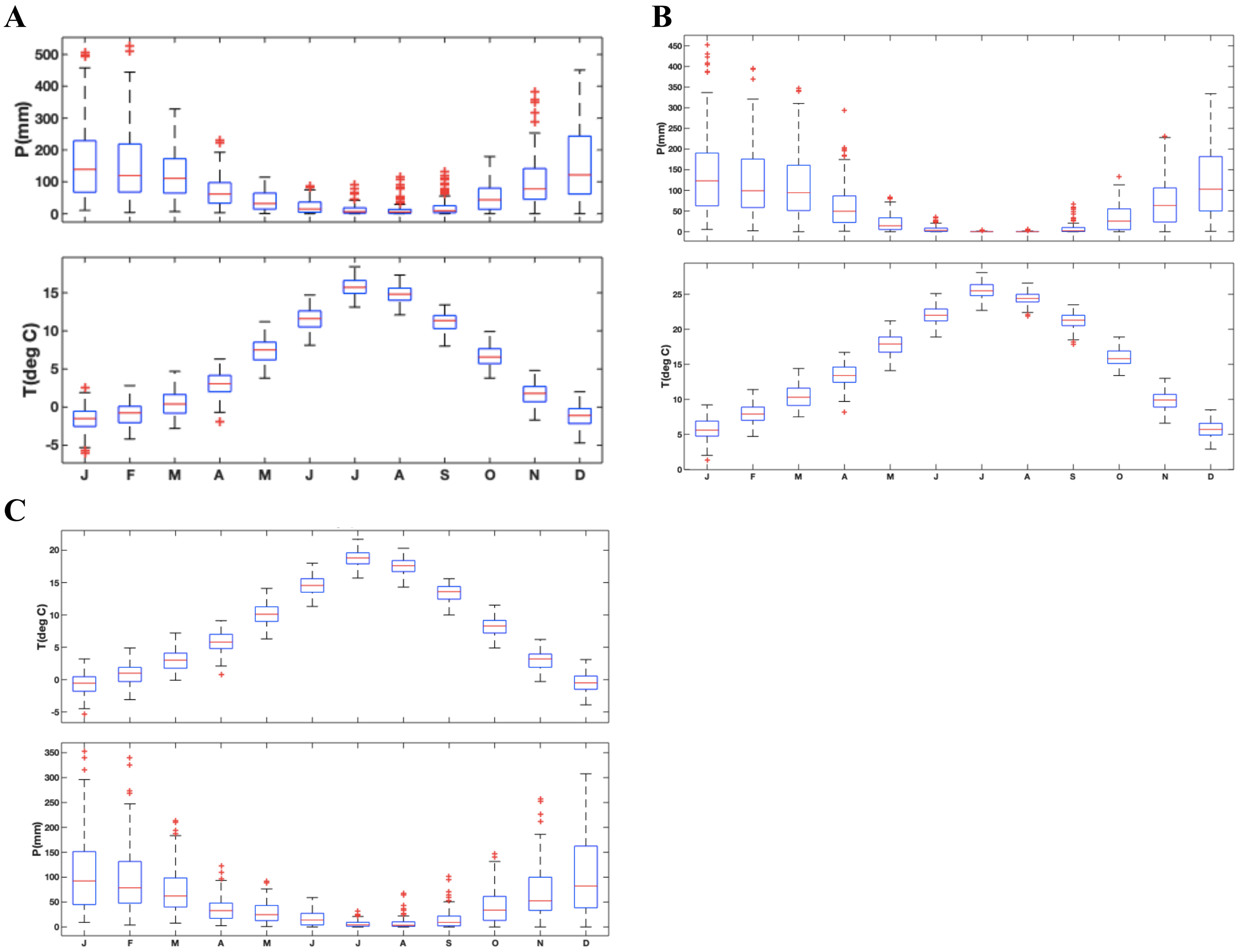

Figure 7 Temperature and precipitation climatology for sites.

Climate data for 3 areas spanning 1901-2018. Temperature (T, deg C) data is averaged for each month and precipitation (P, mm) data is summed monthly. Climate data comes from Climatic Research Unit’s 0.5°x0.5° datasets which averages anomalies over an area. **A)** NRS and NDS climate data (38.000°N, -120.000°W to 38.500°N, -119.500°W) **B)** GRM climate data (37.000°N, -120.000°W to 37.500°N, -119.500°W) **C)** BWF and SNF climate data (39.500°N, -120.500°W to 40.000°N, -120.000°W).

Quantitative Analysis

To assess seasonal climate signals from TRW and BI, we completed data analysis in Matlab, mainly using the tree ring toolbox created by Dr. Dave Meko, specifically the function Seascorr (Meko et al. 2011). The function determines Pearson's r for the tree ring chronology and the climate variable time-series, as well as a partial correlation for a secondary climate variable with the influence from the primary climate variable removed. The function uses 14-month windows from the November in the year before ring formation to the December of the year of growth to determine correlations. Monte Carlo simulations with an adjustable number of simulations is used to determine the significance of correlations. Seasonal correlations are created for four monthly groupings, which are user chosen from 1-14 months. Visual outputs include graphs of tree ring versus climate variable and correlations by month for four monthly groupings.

RESULTS

Tree Ring and Climate Chronologies

Five site chronologies were compiled and detrended, consisting of 211 cores across the sampled and analyzed sites (Table 1). Site GRM spans from 1902 to 2017, with 31 cores in the chronology and a 0.667 mean correlation for individual cores with the master chronology, calculated as the average of the detrended records from individual tree core measurements. Site NRS spans from 1812 to 2018, with 32 cores in the chronology and a 0.605 mean correlation for individual cores with the master chronology. The oldest site is NDS, which spans from 1651 to 2018, with 37 cores in the chronology and a 0.565 mean correlation for individual cores with the master chronology. Site BWF spans from 1839 to 2018, with 12 cores in the chronology and a 0.502 mean correlation for individual cores with the master chronology. Site SNF spans from 1893 to 2018, with 8 cores in the chronology and a 0.431 mean correlation for individual cores with the master chronology.

A nonclimatic signal in NRS compelled us to cut off the last years chronology to compare to climate accurately. The TRW chronology at site NRS has a scale change from 2010-2018 (Fig. 8) that we could not attribute to temperature or precipitation. We could not find any information on historical logging at the site, so we revisited the site to image the stumps we had seen on our first visit. After measuring the ring widths from tree stumps at site NRS, we determined there had been a logging event in 2010. Due to the logging event that affected the competition signal coming from the remaining trees, we use the years 1903 to 2010 to compare NRS to climate.

Tree ring chronologies for both TRW and BI were compared to CRU climate data for 5 sites, with climate data available starting in the year 1901. We used traditional dendroclimatology practices and NDVI climatologies of sites to determine which months of climate were used to compare to the tree ring chronologies. The height of growing season, as estimated by the 3 months with the highest climatological NDVI value, for all sites is in the summer season, from June to September (Fig. 9). To reflect this and make the sites comparable, we used 3 month temperature series from June to August (JJA). We used 12 month precipitation series from the September in the year before ring formation to the August of the year of growth (Sept*-Aug) to capture the start of the rainy season through the time of snow melt.

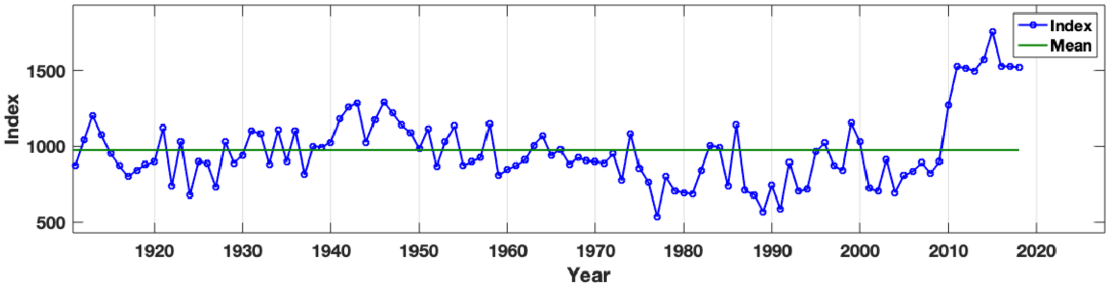

Figure 8 Tree Ring Width time series for site NRS.

The blue line is the detrended tree ring width index from 1910-2018, and the green line is the mean of the index. A scale change starting in 2010 was determined to be a competition signal.

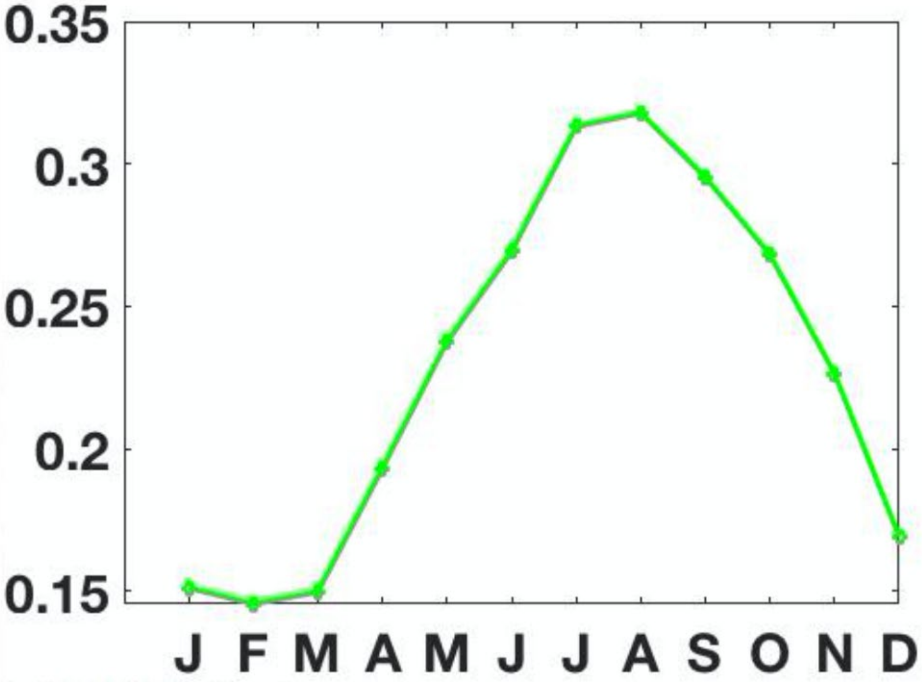

Figure 9 NDVI climatology for site NRS.

Normalized Difference Vegetation Index for a single year shows the peak of growth in the summer. The months with the highest climatological NDVI value are in the summer, from June to September. We chose three months to compare to climate: June, July, and August.

Ring Width Correlations with Climate

In arid locations typical of California, like our study area, precipitation tends to control ring size, which we find to be true at all of our locations. We find that Sept*-Aug (* indicates the month from the previous year) precipitation is positively correlated with TRW at every site (r_{BWF}= 0.33, $p<0.01$, r_{SNF}= 0.11, $p\sim0.10$, r_{GRM}= 0.33, $p<0.01$, r_{NRS}= 0.22, $p<0.01$, r_{NDS}= 0.15, $p<0.10$, Fig. 10, Fig. 11). These relationships vary in strength of signal and significance, but show that moisture availability is important to growth in the study region. At two sites, the relationship between TRW and precipitation was stronger with a period encompassing 10 months of the previous year (March*-February, r_{BWF}= 0.42, $p<0.01$, r_{NDS}= 0.31, $p<0.01$). It is unlikely that the tree can have a memory of rainfall from the previous year, but snowfall from the previous year does affect the amount runoff in the spring of the next year. These two sites may be responding to snow melt from the previous year.

Due to the predicted changes in temperature and precipitation with altitude, we expected to find a relationship between site correlations and site elevations. TRW and precipitation correlations decrease with increasing elevation ($R=-0.89$, $p<0.05$, Fig. 11). Trees at higher elevation sites experience colder temperatures, increased precipitation, and longer snow cover duration (Fig. 7, A, C). Our interpretation of this result is that these high elevation trees are experiencing more stress from cold temperatures than moisture conditions. At lower elevations, trees will have little to no access to moisture during the low precipitation season (Fig. 7, B), and therefore have an enhanced response to year to year changes in precipitation.

Ring Width and JJA temperature are negatively correlated at 4 of 5 sites (r_{BWF}= -0.25, p<0.01, r_{GRM}= -0.33, p<0.01, r_{NRS}= -0.38, p<0.01, r_{NDS}= -0.18, p<0.10, Fig. 12). SNF is the only site that has a positive relationship between TRW and temperature, but it is not significant at a 95% confidence interval (r_{SNF}= 0.20, p<0.10).

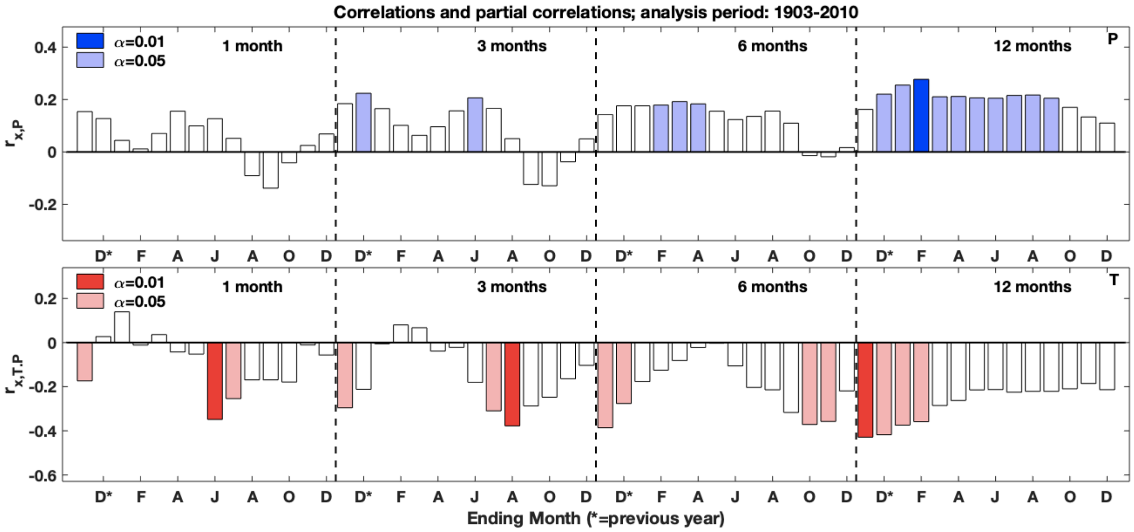

Figure 10 Correlations at site NRS between ring width and precipitation (upper row) and partial correlation with temperature (lower row).

Leftmost panels (a, e) indicate correlations between the tree-ring width site chronology and single-calendar-month time series of climate time series. Months, indicated with an asterisk (*) on the x-axis, show that the correlation is between ring width and climate from the previous calendar year. Lightly colored bars indicate correlations are significant at p<0.05. Dark colored bars indicate correlations are significant at p<0.01. **Second column (b, f)** is the same as the first column, but the climate time series used is a 3-calendar–month average with the x-axis indicating the last month used in the average. **Third column (c, g)** is same as first column, but the climate time series used is a 6-calendar–month average with the x-axis indicating the last month used in the average. **Forth column (d, h)** is same as first column, but the climate time series used is a 12-calendar–month average with the x-axis indicating the last month used in the average.

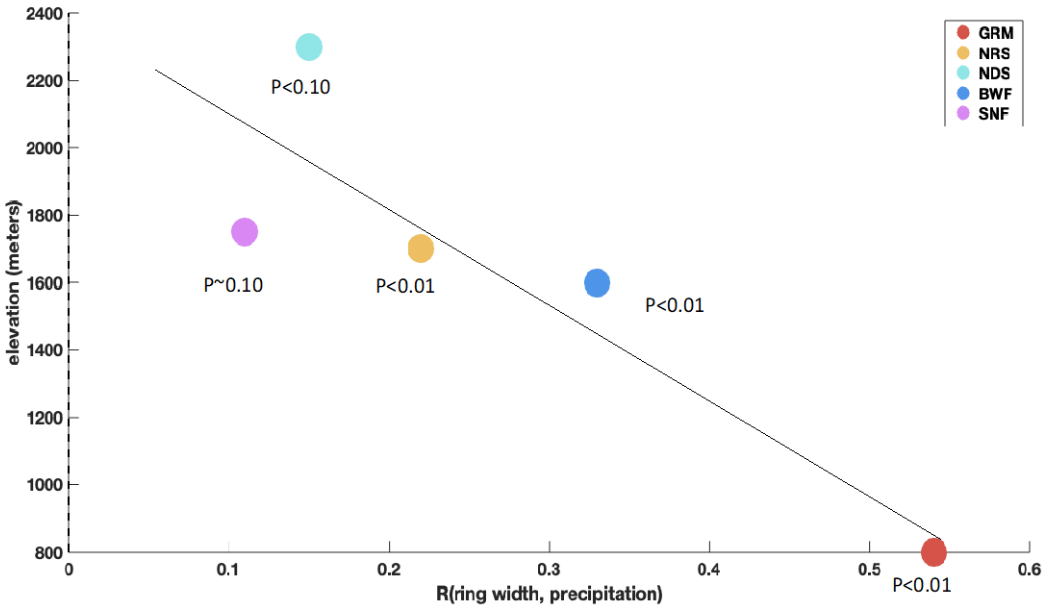

Figure 11 Tree Ring Width and Precipitation correlations compared by elevation. All five sites (listed in legend) have positive correlations between tree ring width and precipitation. Significance of correlations indicated below each point. Strong negative relationship between points ($R=-0.89$, $p<0.05$) demonstrated by a black line.

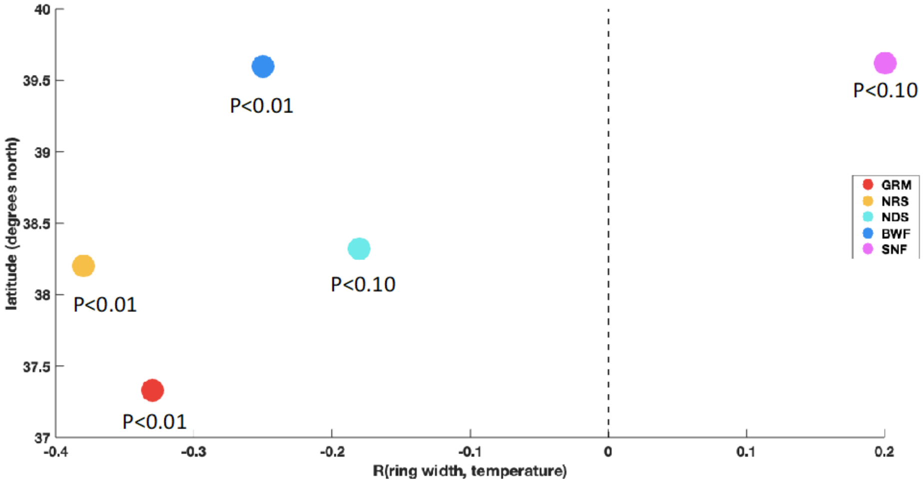

Figure 12 Tree Ring Width and Temperature correlations compared by latitude. Of the five sites, four have a negative relationship between ring width and temperature.

Blue Intensity Correlations with Climate

Previous studies of BI have shown it to have a strong positive relationship with temperature at a variety of locations. In this study, we test whether BI and summer temperature would have a positive relationship in an Mediterranean climate. At our three southern sites we got an anticipated result: BI and JJA temperature correlations are positive ($r_{GRM}= 0.27$, $p<0.01$, $r_{NRS}= 0.47$, $p<0.01$, $r_{NDS}= 0.27$, $p\sim0.15$, Fig. 13, Fig. 14). At our northern sites we had an unexpected result; BI and JJA temperature correlations are negative ($r_{BWF}= -0.20$, $p<0.01$, $r_{SNF}= -0.18$, $p<0.10$).

Of our three sites where relationships between BI and temperature are positive, NRS and NDS cores went through the process of resin extraction, while GRM did not. With the heartwood to sapwood transition intact in GRM, correlations across the series may be degraded, so to test for this we chose to break the series in half. When the GRM time series is broken in half, the second half of the record reports a stronger positive correlation ($r_{GRM}= 0.50$, $p<0.01$, 1961-2017). Splitting the records of the resin extracted sites does not affect correlations for either site. This could indicate that the heartwood to sapwood transition was removed through resin extraction, but we would need an increase in sample depth to verify.

The results of relationship between BI and annual precipitation are reversed from the BI and summer temperature relationship. BI and Sept*-Aug precipitation correlations are positive for the northern sites which exhibited a negative correlation with JJA temperature ($r_{BWF}= 0.16$, $p<0.05$, $r_{SNF}= 0.16$, $p<0.05$, Fig. 15). The aforementioned southern sites that displayed a positive correlation with JJA temperature, have a negative relationship between BI and precipitation, ($r_{GRM}= -0.22$, $p<0.05$, $r_{NRS}= -0.40$, $p<0.01$, $r_{NDS}= -0.04$, $p\sim0.40$). This positive relationship at the northern sites increases by more than double in signal and significance strength for a shorter 6-month period from April to September ($r_{BWF}= 0.35$, $p<0.01$, $r_{SNF}= 0.44$, $p<0.01$). This period encompasses the end of the rainy season and into summer when snow melt may be feeding tree growth. Other studies have found a positive relationship between MXD chronologies from *Pinus* species and a six month season of temperature, with April-September being the optimal time period across the Northern Hemisphere (Briffa et al., 2002).

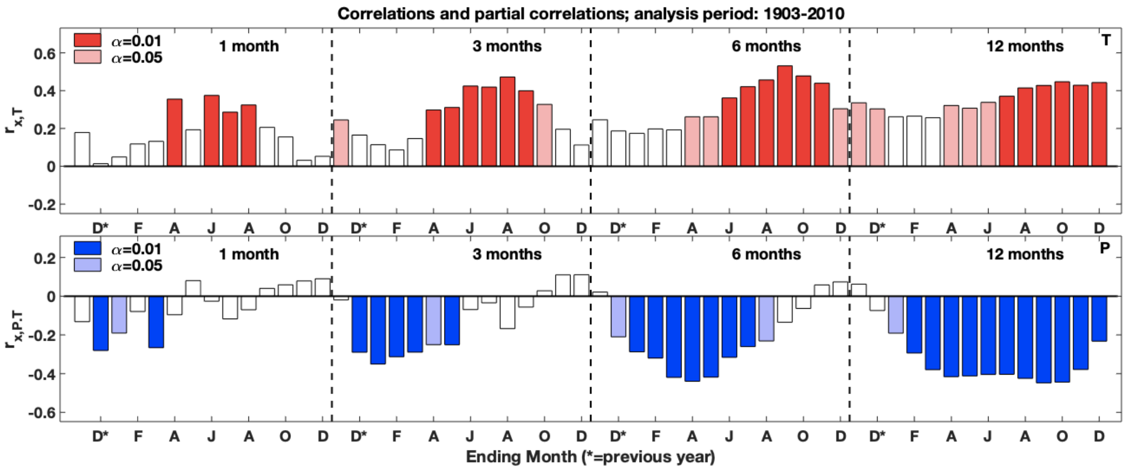

Figure 13 Correlations at site NRS between blue intensity and temperature partial precipitation.

Same as Figure 10, but for blue intensity instead of ring width. Opposite of convention shown as upper row and lower row are switched.

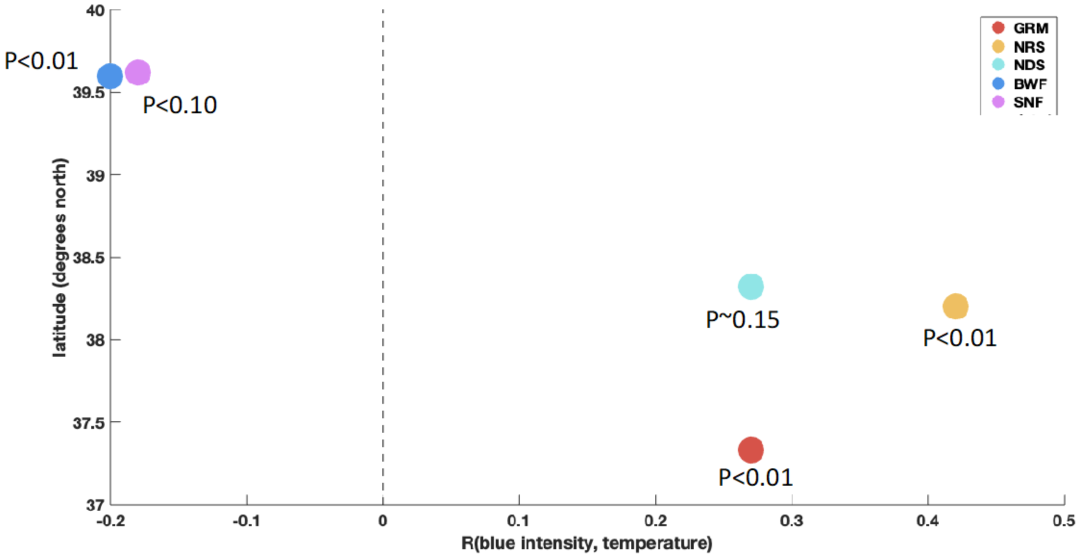

Figure 14 Blue Intensity and Temperature correlations compared to latitude.

Of the five sites, the three southern sites have a positive relationship.

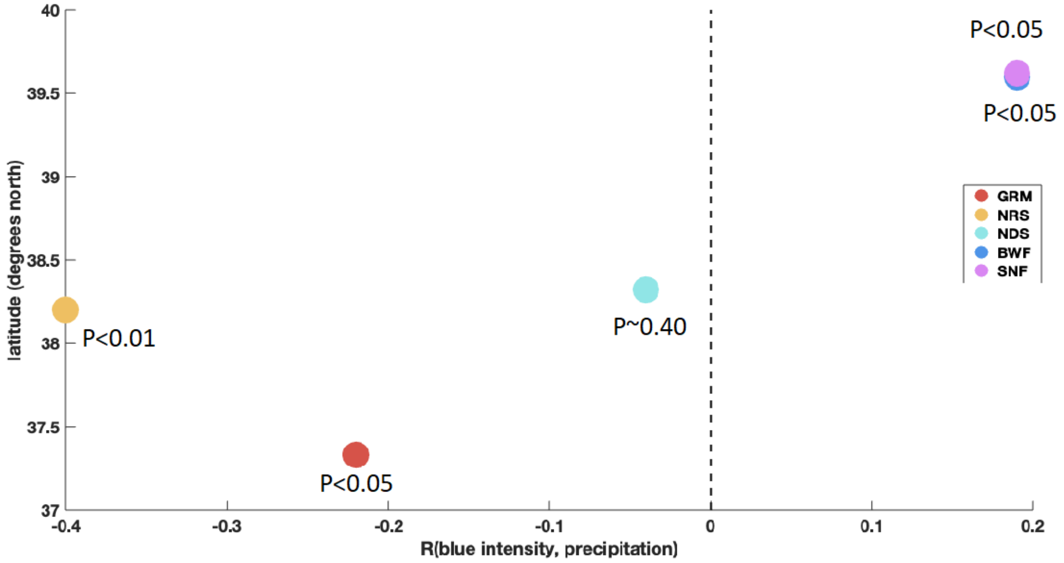

Figure 15 Blue Intensity and Precipitation correlations compared to latitude. Of the five sites, the two the northern sites have a positive relationship.

DISCUSSION

Positive Tree Ring Width and Precipitation Relationship

As expected for moisture limited environments like California, TRW at all sites responds to precipitation. None of our sites were at treeline, so negative relationships between TRW and temperature were anticipated. While annual Sept*-Aug precipitation produces strong and significant results for all sites, the two sites at dissimilar elevations with stronger results from March*-February precipitation demonstrate that snowmelt from the previous year may affect the current year of growth.

Blue Intensity and Precipitation Relationship

BI and temperature were expected to have a positive relationship, but the BI and precipitation positive relationship at our northern sites was surprising. These two northern sites are closer to each other than any other pair of sites in our study in location (5 km apart) and are similar in environment, so we can think of this as a single phenomenon. Why this irregularity is happening at this site may be due to the latitudinal difference, but the climate is cooler at higher latitudes, which would typically lead to increased temperature response.

Mechanisms for Moisture Control of Blue Intensity

We hypothesize that the positive relationship between BI and precipitation at our northern sites is due to difference in mechanisms that control tree growth. Blue intensity presumably arises due to variation in cell lumen area and cell wall thickness. Increased precipitation should increase lumen size, which would lead to a decrease in BI values. This is the mechanism that we predict is occurring in our southern sites, as well as in other BI studies. In order to have an increase in BI values during wet conditions, like we see at our northern sites, the cell walls in the latewood would need to thicken as well. This would follow the source mechanism model, where an increase in precipitation will provide more material for cell wall formation (Table 4).

Logging Event at NRS

We found that a logging event in 2010 at site NRS created a competition signal in our TRW series. The decrease in competition, due to logged trees, made the available trees have more access to resources, such as light, water, or nutrients. The remaining trees showed an increase in TRW, but the signal from BI flattened, and was decreased compared to the previous few decades. With a decrease in competition at this sink limited site, we may expect more water availability to lead to larger lumina, and therefore a decrease in BI. The competition signal from BI should be furthered studied to understand how competition effects latewood color.

Further Study

Reconstructing climate in California with trees is the only way to get annual resolution temperature and precipitation before the 19th century. Previous studies of climate in California have reconstructed precipitation using TRW, but reconstructions of annual temperature are absent in this region. We have found that BI can reconstruct temperature in a moisture-limited environment, but the relationship could use to be strengthened. Our three sites that produced a positive relationship between BI and temperature were all within one latitude degree (37.3-38.3°N) from varying elevations, whereas our northern sites at ~39.5°N did not show a positive relationship between BI and temperature. BI should be expanded at a variety of latitudes to increase temperature signal, with an increase in both sample depth and in study locations. The *Pinus* trees used in our study are the most widespread recorders of climate in our study area, so future studies could continue with this genus across the Sierra Nevadas. Some of the oldest trees in the world are located in California, so continued study of the BI proxy could lead to reconstructions of temperature up to 5,000 years in the past. These Bristlecone Pines are from the same genus as our study species and have been used to reconstruct moisture conditions in California (Ferguson et al., 1983). With such long time records, these trees may experience climate changes and extreme climate events. This could be an issue when reconstructing climate from long tree ring chronologies, as the differing stressors may change which climate variables trees have recorded. Our results show that BI could reconstruct temperature at lower latitudes, so in order to have some confidence that another study would produce similar positive results we would need to choose sites near our study area.

TABLES

Table 1 List of sites.

Site information shown, including site code, name, elevation, latitude, national forest the site is within, the number of crossdated cores and trees, whether cores were resin extracted or not, the years in the master chronology, the mean correlation with the master, and geographical grouping.

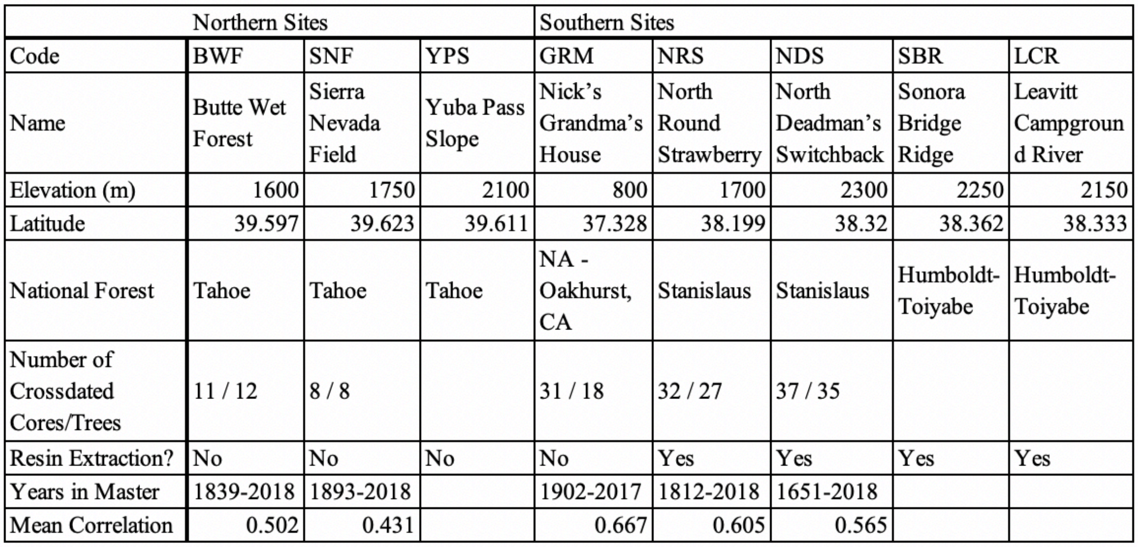

	Northern Sites			Southern Sites				
Code	BWF	SNF	YPS	GRM	NRS	NDS	SBR	LCR
Name	Butte Wet Forest	Sierra Nevada Field	Yuba Pass Slope	Nick's Grandma's House	North Round Strawberry	North Deadman's Switchback	Sonora Bridge Ridge	Leavitt Campground River
Elevation (m)	1600	1750	2100	800	1700	2300	2250	2150
Latitude	39.597	39.623	39.611	37.328	38.199	38.32	38.362	38.333
National Forest	Tahoe	Tahoe	Tahoe	NA - Oakhurst, CA	Stanislaus	Stanislaus	Humboldt-Toiyabe	Humboldt-Toiyabe
Number of Crossdated Cores/Trees	11 / 12	8 / 8		31 / 18	32 / 27	37 / 35		
Resin Extraction?	No	No	No	No	Yes	Yes	Yes	Yes
Years in Master	1839-2018	1893-2018		1902-2017	1812-2018	1651-2018		
Mean Correlation	0.502	0.431		0.667	0.605	0.565		

Table 2 Blue Intensity correlations with climate at each site.

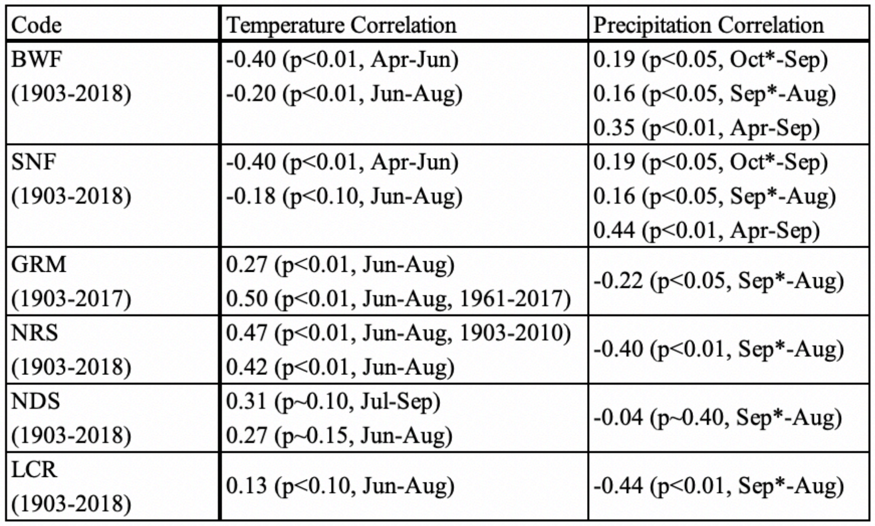

Code	Temperature Correlation	Precipitation Correlation
BWF (1903-2018)	-0.40 (p<0.01, Apr-Jun) -0.20 (p<0.01, Jun-Aug)	0.19 (p<0.05, Oct*-Sep) 0.16 (p<0.05, Sep*-Aug) 0.35 (p<0.01, Apr-Sep)
SNF (1903-2018)	-0.40 (p<0.01, Apr-Jun) -0.18 (p<0.10, Jun-Aug)	0.19 (p<0.05, Oct*-Sep) 0.16 (p<0.05, Sep*-Aug) 0.44 (p<0.01, Apr-Sep)
GRM (1903-2017)	0.27 (p<0.01, Jun-Aug) 0.50 (p<0.01, Jun-Aug, 1961-2017)	-0.22 (p<0.05, Sep*-Aug)
NRS (1903-2018)	0.47 (p<0.01, Jun-Aug, 1903-2010) 0.42 (p<0.01, Jun-Aug)	-0.40 (p<0.01, Sep*-Aug)
NDS (1903-2018)	0.31 (p~0.10, Jul-Sep) 0.27 (p~0.15, Jun-Aug)	-0.04 (p~0.40, Sep*-Aug)
LCR (1903-2018)	0.13 (p<0.10, Jun-Aug)	-0.44 (p<0.01, Sep*-Aug)

Table 3 Tree Ring Width correlations with climate at each site.

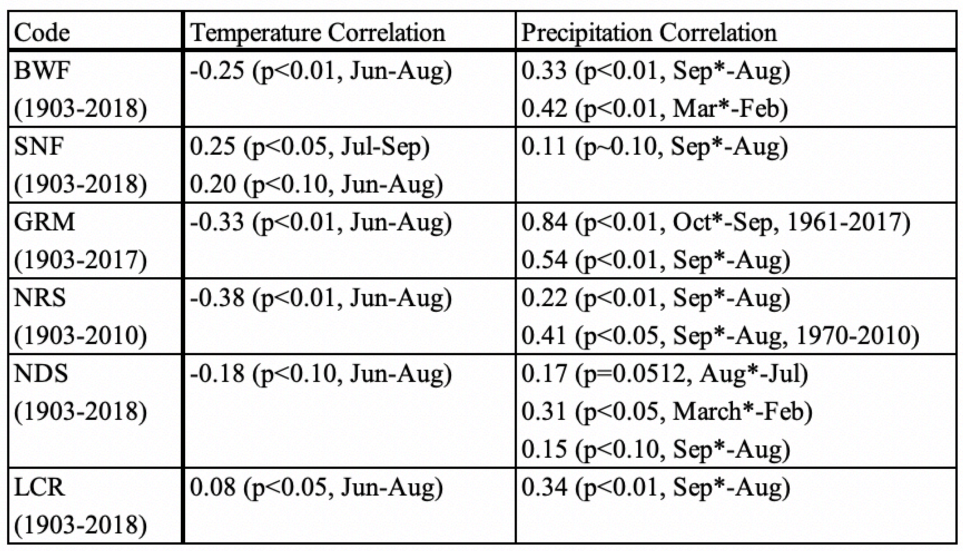

Code	Temperature Correlation	Precipitation Correlation
BWF (1903-2018)	-0.25 (p<0.01, Jun-Aug)	0.33 (p<0.01, Sep*-Aug) 0.42 (p<0.01, Mar*-Feb)
SNF (1903-2018)	0.25 (p<0.05, Jul-Sep) 0.20 (p<0.10, Jun-Aug)	0.11 (p~0.10, Sep*-Aug)
GRM (1903-2017)	-0.33 (p<0.01, Jun-Aug)	0.84 (p<0.01, Oct*-Sep, 1961-2017) 0.54 (p<0.01, Sep*-Aug)
NRS (1903-2010)	-0.38 (p<0.01, Jun-Aug)	0.22 (p<0.01, Sep*-Aug) 0.41 (p<0.05, Sep*-Aug, 1970-2010)
NDS (1903-2018)	-0.18 (p<0.10, Jun-Aug)	0.17 (p=0.0512, Aug*-Jul) 0.31 (p<0.05, March*-Feb) 0.15 (p<0.10, Sep*-Aug)
LCR (1903-2018)	0.08 (p<0.05, Jun-Aug)	0.34 (p<0.01, Sep*-Aug)

Table 4 My conceptual model for the relationship between climate and tree rings.

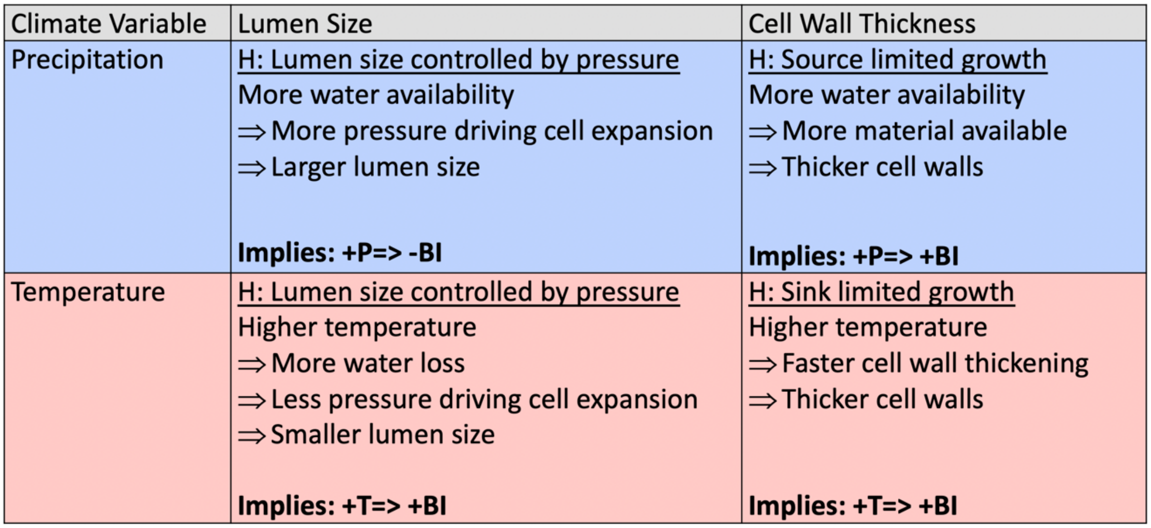

Climate Variable	Lumen Size	Cell Wall Thickness
Precipitation	H: Lumen size controlled by pressure More water availability ⇒ More pressure driving cell expansion ⇒ Larger lumen size **Implies: +P=> -BI**	H: Source limited growth More water availability ⇒ More material available ⇒ Thicker cell walls **Implies: +P=> +BI**
Temperature	H: Lumen size controlled by pressure Higher temperature ⇒ More water loss ⇒ Less pressure driving cell expansion ⇒ Smaller lumen size **Implies: +T=> +BI**	H: Sink limited growth Higher temperature ⇒ Faster cell wall thickening ⇒ Thicker cell walls **Implies: +T=> +BI**

REFERENCES

Babst, F., Frank, D., Büntgen, U., Nievergelt, D., & Esper, J. (2009). Effect of sample preparation and scanning resolution on the blue reflectance of Picea abies. *TRACE Proc, 7*, 188–195.

Babst, F., Wright, W.E., Szejner, P., Wells, L., Belmecheri, S., & Monson, R.K. (2016). Blue intensity parameters derived from Ponderosa pine tree rings characterize intra-annual density fluctuations and reveal seasonally divergent water limitations. *Trees, 30*(4), 1403–1415.

Belokopytova, L.V., Babushkina, E.A., Zhirnova, D.F., Panyushkina, I. P., & Vaganov, E. A. (2018). Pine and larch tracheids capture seasonal variations of climatic signal at moisture-limited sites. *Trees, 33*, 227–242. https://doi.org/10.1007/s00468-018-1772-2

Björklund, J., Gunnarson, B.E., Seftigen, K., Esper, J., & Linderholm, H.W. (2014). Is blue intensity ready to replace maximum latewood density as a strong temperature proxy? A tree-ring case study on Scots pine from northern Sweden. *Clim. Past Discuss, 9*, 5227–5261.

Björklund, J., Gunnarson, B. E., Seftigen, K., Zhang, P., & Linderholm, H. W. (2015). Using adjusted Blue Intensity data to attain high- quality summer temperature information: A case study from Central Scandinavia. *The Holocene, 25*, 547–556.

Björklund, J., Seftigen, K., Schweingruber, F., Fonti, P., von Arx, G., Bryukhanova, M.V., Cuny, H.E., Carrer, M., Castagneri, D., & Frank, D.C. (2017). Cell size and wall dimensions drive distinct variability of earlywood and latewood density in Northern Hemisphere conifers. *New Phytologist, 216*, 728–740.

Björklund, J., von Arx, G., Nievergelt, D., Wilson, R., Van den Bulcke, J., & Günther, B. (2019). Scientific merits and analytical challenges of tree-ring densitometry. *Reviews of Geophysics, 57*, 1224–1264. https://doi.org/10.1029/2019RG000642

Bjorklund J., Gunnarson B., Seftigen K., Esper J., & Linderholm H. (2014). Blue intensity and density from northern Fennoscandian tree rings, exploring the potential to improve summer temperature reconstructions with earlywood information. *Climate of the Past, 10*, 877-885.

Briffa, K.R., Osborn, T.J., Schweingruber, F. H., Jones, P.D., Shiyatov, S.G., & Vaganov E. A. (2002). Tree-ring width and density data around the Northern Hemisphere: Part 1, local and regional climate signals. *The Holocene, 12*(6), 737–757.

Briffa K. R., Schweingruber F. H., Jones P. D., Osborn T. J., Shiyatov S. G., & Vaganov E. A. (1998). Reduced sensitivity of recent tree-growth to temperature at high northern latitudes. *Nature*, *391*, 678-682.

Brown, P.M., Hughes, M.K., Baisan, C.H., Swetnam, T.W., & Caprio, A.C. (1992). Giant sequoia ring-width chronologies from the central Sierra Nevada, California. *Tree-Ring Bulletin*, *52*, 1-14.

Buckley, B. M., Hansen, K. G., Griffin, K. L., Schmiege, S., Oelkers, R., & D'Arrigo, R. D. (2018). Blue intensity from a tropical conifer's annual rings for climate reconstruction: An ecophysiological perspective. *Dendrochronologia, 50*, 10–22. https://doi.org/10.1016/j.dendro.2018.04.003

Bunn, A. G., Graumlich, L. J., Urban, D. L. (2005), Trends in twentieth-century tree growth at high elevations in the Sierra Nevada and White Mountains, USA. *The Holocene, 15*(4), 481–488.

Campbell R, McCarroll D, Loader NJ, Grudd H, Robertson I, & Jalkanen R (2007). Blue intensity in Pinus sylvestris tree rings: developing a new palaeoclimate proxy. *Holocene, 17*, 821–828.

Carver, N. & Stine, A.R. (2018). Recovering Multiple Climate Variables from Single Site Collection of Pinus ponderosa. [Thesis, San Francisco State University].

Cook, E. R. (1985). *A Time Series Analysis Approach to Tree-ring Standardization*. [Doctoral dissertation, University of Arizona].

Cook, E. R., Woodhouse, C. A., Eakin, C. M., Meko, D. M., & Stahle, D. W. (2004). Long-Term Aridity Changes in the Western United States. *Science, 306*(5698), 1015-1018.

Cuny, H. E., Rathgeber, C. B. K., Frank, D., Fonti, P., & Fournier, M. (2014). Kinetics of tracheid development explain conifer tree-ring structure. *New Phytologist, 203*, 1231-1241.

Dannenberg, M. P., & Wise, E. K. (2016). Seasonal climate signals from multiple tree-ring metrics: a case study of Pinus ponderosa in the upper Columbia River basin. *Journal of Geophysical Research: Biogeosciences, 121*, 1178–1189.

Dolanc, C. R., Westfall, R. D., Safford, H. D., Thome, J. H., & Schwartz, M. W. (2013). Growth-climate relationships for six subalpine tree species in a Mediterranean climate. *Can. J. For. Res., 43*(12), 1114-1126.

Dolgova, E. (2016). June–September temperature reconstruction in the Northern Caucasus based on blue intensity data. *Dendrochronologia, 39*, 17–23. https://doi.org/10.1016/j.dendro.2016.03.002

Douglass A.E. (1909). Weather cycles in the growth of big trees. *Mon. Wea. Rev., 37*(6), 225–237.

Ferguson, C.W. & Graybill, D.A. (1983). Dendrochronology of bristlecone pine; a progress report. Radiocarbon, 25(2), 287-288.

Fonti, P., Byukhanova, M.V., Myglan, V.S., Kirdyanov, A.V., Naumova, O.V., & Vaganov E. A. (2013). Temperature-induced responses of xylem structure of *Larix sibirica* (Pinaceae) from the Russian Atlay. *American Journal of Botany, 100*(7), 1332–1343.

Fritts, H. (1966). Growth-Rings of Trees: Their Correlation with Climate. *Science, 154*(3752), 973-979. http://www.jstor.org/stable/1719644

Fritts, H. C., Vaganov, E. A., Sviderskaya, I. V., & Shashkin, A. V. (1991). Climatic variation and tree-ring structure in conifers: empirical and mechanistic models of tree-ring width, number of cells, cell size, cell-wall thickness and wood density. *Clim. Res., 1*, 97-116.

Fuentes, M., Salo, R., Björklund, J., Seftigen, K., Zhang, P., Gunnarson, B., et al. (2018). A 970-year-long summer temperature reconstruction from Rogen, west-central Sweden, based on blue intensity from tree rings. *The Holocene, 28*(2), 254–266. https://doi.org/10.1177/0959683617721322

Graumlich, L. J. (1993). A 1000-Year Record of Temperature and Precipitation in the Sierra Nevada. *Quaternary Research, 39*(2), 249-255.

Griffin D., Meko D. M., Touchan R., Leavitt S., Woodhouse C. A. (2011). Latewood chronology development for summer moisture reconstruction in the US Southwest. *Tree Ring Res, 67*, 87–101.

Holmes, R. L. (1983). Computer-assisted quality control in tree -ring dating and measurement. *Tree-Ring Bulletin, 43*, 69 -78.

Johnson, C., Chhin, S., & Zhang, J. (2017). Effects of climate on competitive dynamics in mixed conifer forests of the Sierra Nevada. *For. Ecol. Manag, 394*, 1–12.

Kaczka, R. J., Spyt, B., Janecka, K., Beil, I., Büntgen, U., & Scharnweber, T. (2018). Different maximum latewood density and blue intensity measurements techniques reveal similar results. *Dendrochronologia, 49*, 94–101. https://doi.org/10.1016/j.dendro.2018.03.005

Kaczka, R. J., Spyt, B., Janecka, K., & Musioł, R. (2017). The blue intensity proxy for>400 years growing season temperature reconstruction from the Tatra Mountains. *TRACE, 15*, 23–30.

Kipfmueller, K. F., & Salzer, M. W. (2010). Linear trend and climate response of five-needle pines in the western United States related to treeline proximity. *Can. J. For. Res., 40*(1), 134-142.

Linderholm, H. W., Björklund, J., Seftigen, K., Gunnarson, B. E., & Fuentes, M. (2015). Fennoscandia revisited: A spatially improved tree-ring reconstruction of summer temperatures for the last 900 years. *Climate Dynamics, 45*(3-4), 933–947.

Ma, L., A. R. Stine, K. A. Simonin. Directional competition at treeline and implications for climate reconstructions. *In Review*.

McCarroll, D., Loader, N. J., Jalkanen, R., Gagen, M. H., Grudd, H., & Gunnarson, B. E. (2013). A 1200-year multiproxy record of tree growth and summer temperature at the northern pine forest limit of Europe. *The Holocene, 23*(4), 471–484. https://doi.org/10.1177/0959683612467483

McCarroll, D., Pettigrew, E., Luckman, A., Guibal, F., & Edouard, J.L. (2002). Blue reflectance provides a surrogate for late- wood density of high-latitude pine tree-rings. *Arctic, Antarctic and Alpine Research 34*, 450–53.

Millar, C.I., Westfall, R.D., Delany, D.L., King, J.C., & Graumlich, L.J. (2004). Response of Subalpine Conifers in the Sierra Nevada, California, U.S.A., to 20th-Century Warming and Decadal Climate Variability. *Arctic, Antarctic, and Alpine Research, 36*, 2, 181–200.

Rathgeber, C.B.K., Cuny, H.E., & Fonti, P. (2016). Biological Basis of Tree-Ring Formation: A Crash Course. *Front. Plant Sci., 7*(734), 1–7.

Rydval, M., Druckenbrod, D. L., Svoboda, M., Trotsiuk, V., Janda, P., & Mikoláš, M. (2018). Influence of sampling and disturbance history on climatic sensitivity of temperature-limited conifers. *The Holocene, 28*(10), 1574–1587. https://doi.org/10.1177/0959683618782605

Rydval, M., Gunnarson, B. E., Loader, N. J., Cook, E. R., Druckenbrod, D. L., & Wilson, R. (2017). Spatial reconstruction of Scottish summer temperatures from tree rings. *International Journal of Climatology, 37*(3), 1540–1556.

Rydval, M., Larsson, L.-Å., McGlynn, L., Gunnarson, B. E., Loader, N. J., Young, G. H. F., & Wilson, R. (2014). Blue intensity for dendroclimatology: Should we have the blues? Experiments from Scotland. *Dendrochronologia, 32*(3), 191–204.

Rydval, M., Loader, N. J., Gunnarson, B. E., Druckenbrod, D. L., Linderholm, H. W., & Moreton, S.G. (2017). Reconstructing 800 years of summer temperatures in Scotland from tree rings. *Climate Dynamics, 49*(9-10), 2951–2974. https://doi.org/10.1007/s00382- 016-3478-8

Schweingruber, F.H., Fritts, H.C., Bräker O.U., Drew L.G., & Schär, E. (1978). The X-ray technique as applied to dendroclimatology. *Tree Ring Bull, 38*, 61–91.

Scuderi, L. A. (1993), A 2000-Year Tree Ring Record of Annual Temperatures in The Sierra Nevada Mountains. *Science, 259*(5100), 1433-1436.

Sheppard, P. R., Graumlich, L. J., & Conkey, L. E. (1996). Reflected-light image analysis of conifer tree rings for reconstructing climate. *The Holocene, 6*(1), 62–68.

Sheppard, P. R. (2007). Overcoming extraneous wood color variation during low-magnification reflected-light image analysis of conifer tree rings. *Wood and fiber science, 31*(2), 106–115.

Stine, A.R., & Huybers, P. (2017). Implications of Liebig's law of the mini- mum for tree-ring reconstructions of climate. *Environ Res Lett, 12*(11),114018.

Tene, A., Tobin, B., Dyckmans, J., Ray, D., Black, K., & Nieuwenhuis, M. (2011). Assessment of tree response to drought: Validation of a methodology to identify and test proxies for monitoring past environmental changes in trees. *Tree physiology, 31*(3), 309–322.

White, A.C., Rogers, A., Rees, M., & Osborne, C.P. (2015). How can we make plants grow faster? A source–sink perspective on growth rate. *Journal of Experimental Botany, 67*(1), 31–45.

Wilson, R., Rao, R., Rydval, M., Wood, C., Larsson, L. Å., & Luckman, B. H. (2014). Blue intensity for dendroclimatology: The BC blues: A case study from British Columbia, Canada. *The Holocene, 24*(11), 1428–1438.

Wilson, R., Wilson, D., Rydval, M., Crone, A., Büntgen, U., Clark, S., Ehmer, J., Forbes, E., Fuentes, M., Gunnarson, B. E., & Linderholm, H. W. (2017). Facilitating tree-ring dating of historic conifer timbers using Blue Intensity. *J. Archaeol. Sci., 78*, 99–111. https://doi.org/10.1016/j.jas.2016.11.011